# VISCOUS EFFECTS ON STATIC PRESSURE DISTRIBUTION FOR A SLENDER CONE AT A NOMINAL MACH NUMBER OF 5.8

Thesis by

Lawrence C. Baldwin

Lieutenant, U.S. Navy

In Partial Fulfillment of the Requirements

For the Degree of

Aeronautical Engineer

California Institute of Technology

Pasadena, California

1955

## ACKNOWLEDGMENTS

The author wishes to express his appreciation to Professor Lester Lees and to Dr. H. T. Nagamatsu for their interest and guidance during the course of this investigation. Sincere thanks are extended to the staff of the GALCIT Hypersonic Wind Tunnel for their cooperation and assistance, to Mr. Wm. Sublette of the GALCIT Machine Shop who skillfully constructed the model, and to Mrs. H. Van Gieson and Mrs. Fae Kelly, for their expert assistance in the preparation of the final manuscript.

ABSTRACT

An experimental investigation was conducted in the GALCIT Hypersonic Wind Tunnel, Leg No. 1, to determine the static pressure distribution on a cone with $5^{\circ}$ semivertex angle at a nominal Mach number of 5.8.

This investigation was concerned with the effect of hypersonic boundary layer-shock wave interaction on the pressure at the cone surface. Pressure distributions were measured for three values of Reynolds numbers per inch and a comparison was made with theoretically calculated pressure distributions.

The influence of viscosity in hypersonic flow was demonstrated by an induced pressure rise of approximately 45% above theoretical inviscid pressure for the lowest Reynolds number tested.

TABLE OF CONTENTS

## LIST OF FIGURES

## LIST OF SYMBOLS

The subscript "1" refers to conditions in the free stream ahead of the conical shock, and the subscript "2" refers to local conditions on the cone surface. Stagnation values are denoted by the subscript "0". A second subscript "i" refers to inviscid flow values.

| | |
|---|---|
| $C_c$ | constant of proportionality in viscosity-temperature relation $\mu/\mu_2 = C_c(T/T_2)$ |
| $c_p, c_v$ | specific heats at constant pressure and volume |
| K | hypersonic similarity parameter, $M_1 \theta_c$ |
| k | coefficient of thermal conductivity |
| M | Mach number |
| p | pressure |
| Pr | Prandtl number, $c_p \mu/k$ |
| $Re_x$ | Reynolds number based on distance x, u x/ |
| T | absolute temperature |
| u,v | velocity components parallel and normal to cone surface, respectively |
| x,y | coordinates parallel and normal to cone surface with origin at apex |
| $\gamma$ | ratio of specific heats $c_p/c_v$ |
| $\delta^*$ | boundary layer displacement thickness |
| $\theta$ | flow deflection angle |
| $\theta_c$ | cone semi-vertex angle |
| $\mu$ | coefficient of viscosity |
| $\rho$ | mass density |
| $\lambda$ | ratio defined by Eq. (4) |
| $\bar{\chi}_c$ | induced pressure field parameter, $\sqrt{C_c}\ \dfrac{M_2^3}{\sqrt{Re_{x_2}}}$ |

# I. INTRODUCTION

With the advent of hypersonic flight, attention is quite naturally directed to the complicated problems associated with such high speeds. One aspect of hypersonic flight is the complex "interaction" between the viscous and inviscid properties of the fluid. The boundary layer is considerably thicker at hypersonic speeds, and in addition, the shock wave lies much closer to the edge of the boundary layer. The deflection of the streamlines induced by the boundary layer amounts to a significant change in the shape of the body, and this in turn affects the shape of the shock wave. Because of the interaction, the actual pressure distribution over a body in hypersonic flight may vary considerably from that predicted by inviscid theory.

The problem of the effect of the interaction between shock wave and boundary layer has been the subject of a number of theoretical and experimental investigations (Cf. Refs. 1 to 4). Since only limited data on pressure distributions in the hypersonic speed range are available, an investigation to determine the static pressure distribution over an unyawed cone was undertaken. No attempt was made to formulate new theory. It was desired to obtain the information so that it would be available for further studies.

This investigation was conducted at a nominal Mach number of 5.8 in Leg No. 1 of the GALCIT Hypersonic Wind Tunnel. The design and materials of the model were chosen so that it might later be used in Leg No. 2, at a Mach number of 10.

## II. EQUIPMENT AND PROCEDURE

### A. Wind Tunnel Description

The experimental program was conducted in the GALCIT 5" x 5" Hypersonic Wind Tunnel, Leg No. 1. This is a continuously operating, closed return type tunnel with the required compression supplied by five stages made up from thirteen Fuller Rotary Compressors. When necessary an additional compressor stage consisting of Ingersoll Reciprocating Compressors may be utilized. The compressors and valving in the system were operated from a remote control panel adjacent to the test section.

The air heating system consisted of a multiple-pass heat exchanger and used superheated steam as a heating medium.

Drying of the air was accomplished by use of a 2200 pound bed of silica gel. This was reactivated by an integral blower heater condenser system. The maximum water content was kept below 100 ppm (parts per million) by weight.

Oil removal was accomplished by use of cyclone separators following each compression stage and by finely divided carbon canistors, porous carbon filter blocks and a fiber glass filter. The presence of oil in the air was due to the lubrication system required by the rotary compressors. Air used during the tests contained approximately 2.5 ppm of oil by weight.

The nozzle blocks were designed by the Foelsch method and corrected for an estimated boundary layer displacement thickness. Static pressure orifices were installed at one inch intervals along the top and bottom nozzle blocks. A comparison of the actual pressure in the

test rhombus was made with calibration data from tunnel-empty pressure surveys.

A schematic diagram of the plant is shown in Fig. 1.

## B. Instrumentation

All static pressures were measured by a 32-tube vacuum-referenced manometer using DC-200 silicone fluid. A Tate-Emery nitrogen balanced gage measured tunnel stagnation pressure; this pressure was controlled within $\pm$.04 psi by a Minneapolis Honeywell Brown controller.

Stagnation temperature was measured by a thermocouple probe located one inch upstream of the nozzle throat and controlled by a Brown Controller. Other temperatures necessary for plant operation were recorded by a 20 point Leeds and Northrup recorder.

A schlieren system using a BH-6 steady source was used for the schlieren photographs.

## C. Model Description

The basic model was a slender cone with semivertex angle of $5^{\circ}$. Two separate models were made; both were constructed in the same manner, although the orifice locations were different. Tests were made on both models; however, all the data presented in this report were taken from runs made on the second model.

The model was constructed in two parts, as shown in Figs. 2 and 3. The conical frustrum was 4.72" long, with large base diameter of 1 inch and small base diameter of .175 inches. Into the small base could be fitted the separate conical tips which were 1 inch in length. The

over-all length of the assembled cone was 5.74 inches.

A set of five cone tips were made, four of which had a single pressure orifice located at various distances from the apex. The fifth tip had two orifices. The orifice locations, measured along a ray of the cone with origin at the vertex, were as follows:

| Orifice | Location |
|---|---|
| 1 | .098" |
| 2 | .128" |
| 3 | .174" |
| 4 | .250" |
| 5 | .392" |
| 6 | .696" |
| 7 | 1.570" |
| 8 | 2.780" |
| 9 | 4.000" |

Additional orifices were installed at 90° intervals around the circumference as shown in Fig. 2. A thermocouple was located 4.5" from the apex.

Orifice diameters for the cone tips were of necessity very small, ranging from .004" for the first to .013" for the fifth. Orifices installed on the cone frustrum were .027". Specifications are listed in Fig. 2.

The model was machined from stainless steel, and polished. The cone tips were surface finished after assembly, so that the joint was quite smooth. The model was supported by a hollow sting approximately 14" long and $\frac{1}{2}$" in diameter. Tubing was led out through the sting. One orifice was installed in the sting very near the base of the cone to determine the base pressure.

The model installed in the tunnel is shown in Fig. 4. The sting

was fitted into a collar, secured by set screws, and suspended from a pair of vertical actuators which could be positioned by controls outside the tunnel. This permitted the model angle of attack to be adjusted. In addition a small adjustment in yaw was possible.

Leak tests were conducted before each run. Time responses of the small orifices were quite long.

## D. Tunnel Calibration

Static pressures in the tunnel were measured by orifices installed along the top and bottom nozzle blocks. These were compared with original nozzle calibration data for each run. Also static pressure surveys were made over the test rhombus to determine axial static pressure variations; measurement of tunnel stagnation pressure with the assumption of isentropic flow permitted determination of free stream Mach number.

A plot of tunnel empty static pressure over the region occupied by the model is shown in Fig. 12.

## E. Test Procedure

### 1. Static Pressure Distribution

The model was installed on the tunnel centerline as shown in Fig. 4. The distance between the base of the cone and the support collar was 3.5". The orifices located about the circumference were used to position the model at zero angle of attack. Tests were conducted as follows:

| $T_o$(°F) | $P_o$(psig) | Re/in |
|---|---|---|
| 225 | 80 | $23.2 \times 10^4$ |
| 225 | 32.6 | 12.1 |
| 225 | 10 | 6.6 |

A schlieren photograph taken during the test is shown in Fig. 5.

2. Additional Tests

Tests were also conducted with the model located off the centerline and at different axial positions. The distance between the base of the cone and the collar was at first set at 1.5"; the collar then installed was 1" in diameter. At this position a pressure rise was noted over the last two orifices. A new support collar 3/4" in diameter was installed and the distance from base to collar was increased in increments. Beyond 3.5" there seemed to be no effect on the last two orifices so the cone location was fixed at this point.

Tests at $\frac{1}{2}$" above and below the centerline showed no appreciable change in the pressures sensed at the orifices.

At $P_o$ = 80 psig the angle of attack was varied over a small range of three degrees in one degree increments to determine the effect of yaw on pressure distribution.

## III. DISCUSSION OF RESULTS

### A. Surface Pressure Distribution Data

The pressure distributions are presented in Figs. 7 to 10. The data were plotted in the following manner: first, as the ratio of measured pressure to stagnation pressure versus the linear distance along a ray of the cone; and second, as the per cent pressure rise above the theoretical inviscid pressure versus the parameter $1/\sqrt{Re_{x_2}}$. Reynolds number was based on the local conditions on the cone and on the distance from the apex. The theoretical inviscid surface pressure to stagnation pressure ratio was computed by taking the tunnel empty survey data corresponding to a point on the cone and calculating the conditions behind the conical shock. This gave the inviscid pressures shown in Figs. 7, 8, and 9.

The plot of induced pressure increment shows a maximum induced pressure rise of approximately 45% for the lowest Reynolds number tested. The scatter at the higher values of stagnation pressures was rather small, but was considerably larger at the lowest pressure. Response times were quite long for the tip orifices, requiring approximately one hour for each point.

The plot against $1/\sqrt{Re_{x_2}}$ seemed to bring the data at the various stagnation pressures into good agreement. However, when extrapolated to infinite Reynolds number, the plot passed slightly below the inviscid pressure. The initial tests at different axial positions indicated that the model support was influencing the surface pressure near the base, but modification of the support collar and increasing the distance from the cone base to support at least decreased this effect. Although

Harkins (Ref. 8) indicated that the support interference could possibly be felt for string lengths less than seven inches, the physical limitations and other considerations prevented the location of the model with this length of sting. Base pressures measured during the tests were considerably lower than the surface pressures at the orifices nearest the base. Hammitt and Bogdonoff (Ref. 5) noted a similar effect on pressures near the base of a cone during tests in helium at Mach number 13; it was attributed to trailing edge disturbances propagating forward through the boundary layer.

The thickness of the leading edge of a flat plate has been shown to exert some influence on the induced pressure. Since the effect of the radius at the apex of the cone is probably similar, a microscopic examination of the cone tips was made which showed some inaccuracies. Some microphotographs of the tips are shown in Fig. 6. The diameter at the apex of three of the tips was approximately .001"; one had a diameter of approximately .0015" and the last had a diameter of .0003". These distances were ten to twelve times the mean free path of the flow at $P_o$ = 10 psig, except the latter which was about four times mean free path. In addition the angles were not exact very near the tip. It is considered probable that these inaccuracies account for some of the scatter, especially at the lowest value for $P_o$.

The effect of yaw on the cone was least minimized by adjusting the position of the cone so that the pressures at the diametrical locations were equalized. However, a tunnel survey showed that small variations in flow direction existed in the test rhombus.

B. Comparison with Theory

A number of attempts have been made to treat theoretically the problem of hypersonic boundary layer--shock wave interaction. Lin, Schaaf, and Sherman (Ref. 1) developed a simple relation for the induced pressure distribution by using the linearized solution given by Laitone (Ref. 11) for flow over an infinite slender body of revolution, and applying the tangent cone approximation to the composite body of cone plus the boundary layer displacement thickness. Talbot (Ref. 6) compared their results with data obtained for low density flow over a $5^{\circ}$ cone at a nominal Mach number of 4.0. The limitations of this theory were quite severe however, and it was not considered applicable to this experiment.

The theoretical work of Lees and Probstein seemed to offer a better basis for comparison. Probstein (Ref. 9) considered the problem of the steady hypersonic viscous flow over an unyawed cone. The case of "weak" interaction was treated, where it was assumed that the shock exerted only a small influence and the induced pressure gradients were considered to be perturbations on a uniform flow. It was pointed out that, in general, a rotational characteristics computation would be required to compute the inviscid pressure field. However, the tangent cone approximation was adopted, and the pressure was written as a Taylor's series expansion in powers of $d\delta^*/dx$ as follows:

$$\frac{P_2}{P_{2_i}} = 1 + \frac{1}{(P_{2_i}/P_i)} \left[\frac{d\left(\frac{P_2}{P_i}\right)}{d\theta}\right]_{\theta=\theta_c} \left(\frac{d\delta^*}{dx}\right) + \frac{1}{2!} \frac{1}{(P_{2_i}/P_i)} \left[\frac{d^2\left(\frac{P_2}{P_i}\right)}{d\theta^2}\right]_{\theta=\theta_c} \left(\frac{d\delta^*}{dx}\right)^2 + \cdots \qquad (1)$$

The change of displacement thickness, $d\delta^*/dx$, for zero pressure gradient was then calculated as the first step in an iteration process. $d\delta^*/dx$ was obtained for a body of revolution by using the Mangler transformation and was given by

$$\frac{d\delta^*}{dx} = \frac{d_c}{\sqrt{3}} \sqrt{C_c} \frac{M_2^2}{\sqrt{Re_{x_2}}} \tag{2}$$

where the quantities $d_c$ and $C_c$ were the boundary layer parameter defined as a function of the gas properties, and the proportionality constant in the assumed viscosity-temperature relation, respectively. For air, $C_c$ was approximately equal to unity (Ref. 10). Also for an insulated body with Pr = .725, $d_c$ was given by the approximate relation

$$d_c \simeq .556 (\gamma - 1).$$

It was also pointed out that the coefficients of $d\delta^*/dx$ in Eq. (1) could be evaluated numerically from the inviscid Taylor-Maccoll solutions. However, for values of the hypersonic similarity parameter $K = M \theta_c \gg 1$, algebraic relations were obtained for the coefficients as functions of K and $\gamma$. Eq. (1) was then written as follows:

$$P_2/P_{2i} = 1 + F_1(K)\, d_c \bar{\chi}_c + F_2(K)\, d_c^2 \bar{\chi}_c^2 \tag{3}$$

where $\bar{\chi}_c$ was the induced pressure field parameter defined by

$$\bar{\chi}_c = \gamma C_c \frac{M_2^3}{\gamma Re_{x_2}} .$$

The functions $F_1(K)$ and $F_2(K)$ were computed and plotted for $K \gg 0.5$; however, the approximation was not considered satisfactory for $K < 1$.

The accuracy of the tangent cone approximation was examined by Lees in Ref. 12. By comparing the tangent cone approximation with characteristics solutions a first order "correction factor", $\lambda$ , was evaluated for various values of K. $\lambda$ was defined by

$$\lambda = \frac{\left[\frac{d\left(\frac{P_2}{P_1}\right)}{d\theta}\right]_{\text{"exact"}}}{\left[\frac{d\left(\frac{P_2}{P_1}\right)}{d\theta}\right]_{\text{"Tangent Cone"}}} \tag{4}$$

For purposes of comparison with this experiment, Eq. (4) was applied to Eq. (1), giving (dropping higher order terms)

$$\frac{P_2}{P_{2_i}} = 1 + \frac{\lambda}{(P_{2_i}/P_1)}\left[\frac{d\left(\frac{P_2}{P_1}\right)}{d\theta}\right]_{\theta=\theta_c}\left(\frac{d\delta^*}{dx}\right) \tag{5}$$

or in terms of the parameter $\bar{\chi}_c$.

$$\frac{P_2}{P_{2_i}} = 1 + \left\{\frac{\lambda}{(P_{2_i}/P_1)}\left[\frac{d\left(\frac{P_2}{P_1}\right)}{d\theta}\right]_{\theta=\theta_c}\frac{d_c}{\sqrt{3}}\frac{M_1}{M_2}\right\}\bar{\chi}_c \tag{5a}$$

In this experiment K = 0.5; in view of the fact that the functions $F_1(K)$ and $F_2(K)$ did not hold for $K < 1$ the coefficients of $d\delta^*/dx$ in Eq. (1) were calculated numerically by Ref. 7. $M_2$ and $Re_{x_2}$ were based on local conditions "far" downstream from the cone apex. $\lambda$ , obtained from Ref. 12, was 1.19. Eqs. (5a) and (1) (first order terms) are compared with the experimental data in Fig. 11. In general the data are somewhat higher than theoretical predictions. As mentioned previously the cone tips were not perfectly sharp; all had finite radii at the apex which were greater than the mean free path. Hammitt and Bogdonoff in Ref. 5 state that the experimental realization of a sharp leading edge might be obtained if the leading edge radius were a small percentage of

the mean free path. Since the theory does not consider the effect of a finite radius at the cone apex or the effect of a radical change in the shape of the shock wave in the vicinity of the apex, this result is not unexpected.

## IV. CONCLUSIONS

The results of the investigation of pressure distribution on a $5^{\circ}$ cone at a nominal Mach number of 5.8 indicate the following:

(1) The induced pressure was approximately 45% greater than theoretical inviscid pressure for the lowest Reynolds number tested.

(2) The use of the parameter $1/\sqrt{Re_{x_2}}$ correlated the data taken at various stagnation pressures quite well.

(3) The measured pressures nearest the apex were somewhat higher than theoretically predicted pressures. The unknown influence of the region in the immediate vicinity of the apex points to the need for further tests to determine this effect.

## REFERENCES


1. Lin, T. C., Schaaf, S. A., and Sherman, F. S.: Boundary Layer Effect on the Surface Pressure of an Infinite Cone in Supersonic Flow. University of California, Institute of Engineering Research, Berkeley, California, Report No. HE-150-80, 5 March 1951.

2. Li, T. Y. and Nagamatsu, H. T.: Shock Wave Effects on the Laminar Skin Friction on an Insulated Flat Plate at Hypersonic Speeds. California Institute of Technology, Guggenheim Aeronautical Laboratory, Memorandum No. 9, Contract No. DA-04-495-Ord-19, July 1, 1952.

3. Lees, L.: Influence of the Leading Edge Shock Wave on the Laminar Boundary Layer at Hypersonic Speeds. California Institute of Technology, Guggenheim Aeronautical Laboratory, Technical Report No. 1, Contract No. DA-04-495-Ord-19, 15 July 1954.

4. Lees, L. and Probstein, R. F.: Hypersonic Flows of a Viscous Fluid. Monograph, unpublished.

5. Hammitt, A. G. and Bogdonoff, S. M.: A Study of the Flow about Simple Bodies at Mach Numbers from 11 to 15. Princeton University, Aeronautical Engineering Department, Report No. 277, Contract AF 33(038)-250, September, 1954.

6. Talbot, L.: Viscosity Corrections to Cone Probes in Rarefied Supersonic Flow at a Nominal Mach Number of 4. NACA Technical Note No. 3219, November, 1954.

7. Kopal, Zdenek: Tables of Supersonic Flow Around Cones. Massachusetts Institute of Technology, Technical Report No. 1, 1947.

8. Harkins, W. D.: Base Pressure and Static Pressure for a Cone Cylinder at a Nominal Mach Number of 5.8. California Institute of Technology, Guggenheim Aeronautical Laboratory, Memorandum No. 19, Contract No. DA-04-495-Ord-19, 20 July 1954.

9. Probstein, R. F.: Interacting Hypersonic Laminar Boundary Layer Flow over a Cone. Technical Report AF 2798/1, Division of Engineering, Brown University, Providence, Rhode Island, March, 1955.

10. Keyes, F. G.: Heat Conductivity, Viscosity, Specific Heat and Prandtl Number for Thirteen Gases. Project SQUID Technical Report 37, Massachusetts Institute of Technology, 1 April 1952.

11. Laitone, E. V.: The Linearized Subsonic and Supersonic Flow about Inclined Slender Bodies of Revolution. Journal of the Aeronautical Sciences, Vol. 14, No. 11, pp. 631-642, November, 1947.

12. Lees, L.: Hypersonic Flows. Paper to be presented at the Fifth International Aeronautical Conference (I.A.S. - R. Ae. S.), Los Angeles, California, 20 June 1955.

# APPENDIX A

## ACCURACY ANALYSIS

Magnitudes of random errors were estimated by considering reproducibility of observations, sensitivity of the scale, and associated reading errors. For the experimentally measured quantities these errors were as follows:

| Measurement | Estimated Maximum Error |
|---|---|
| Surface pressure, $p_2$ | $\pm$0.4 mm Silicone |
| Stagnation pressure, $p_o$ | less than 0.5% |
| Tunnel static pressure, $p_1$ | $\pm$0.2 mm Silicone |

The accuracy of the computed values based on estimated errors in individual measurements is as follows:

| Quantity | Maximum Error |
|---|---|
| Pressure ratio, $p_2/p_o$ | $\pm$2.5% |
| Pressure ratio, $p_{2_1}/p_o$ | $\pm$2 % |
| Reynolds number, Re | $\pm$1 % |
| $\bar{X}_c$ | $\pm$2 % |

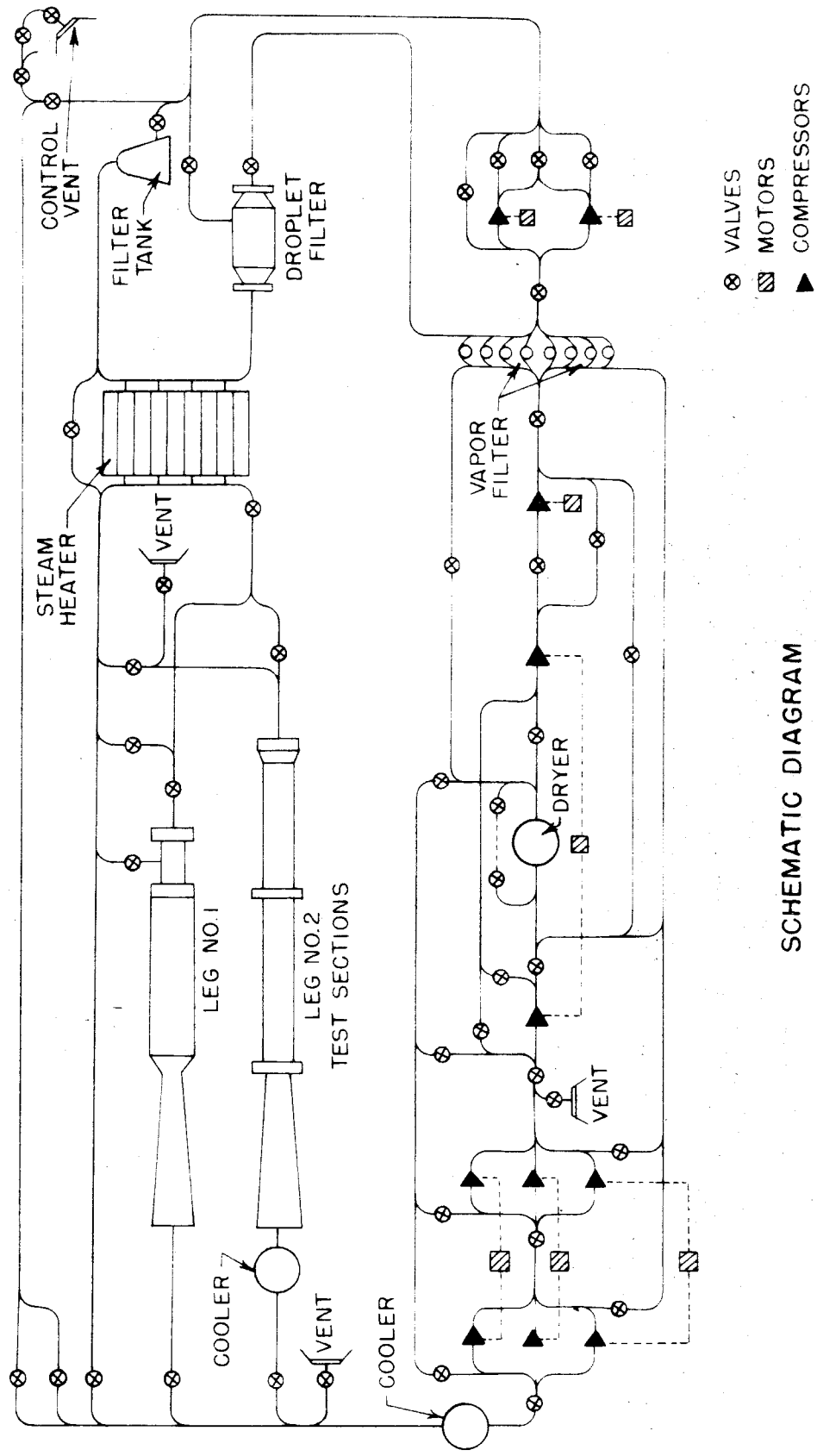


SCHEMATIC DIAGRAM

OF GALCIT 5x5in. HYPERSONIC WIND TUNNEL INSTALLATION

FIG. 1

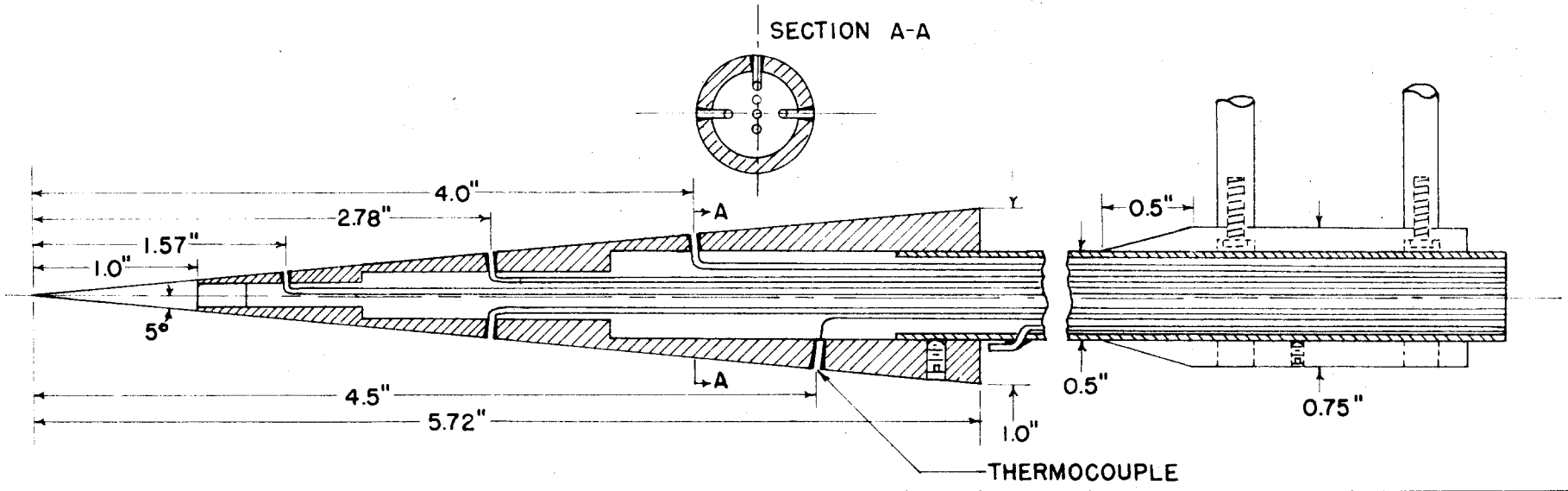


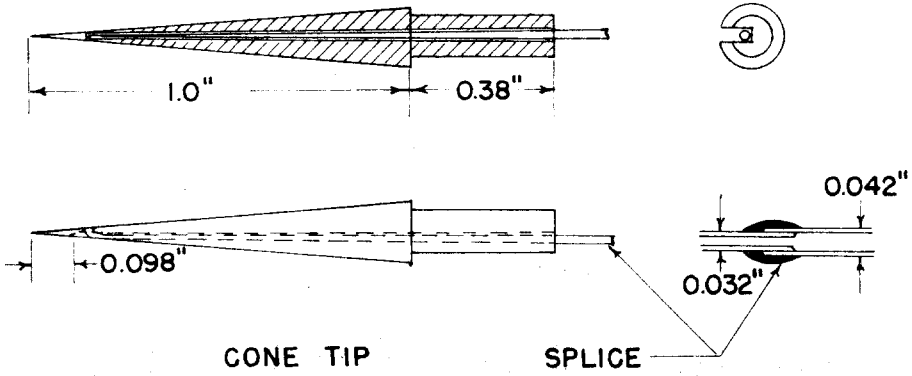


CONE TIP
(SET OF FIVE)
SCALE 2:1

| Tip No. | Orifice No. | Distance from Apex | Orifice Diameter | Tubing | Remarks |
|---|---|---|---|---|---|
| Cone Frustrum | 1 | .098" | .004" | .016"O.D. | |
| | 2 | .128 | .008 | .016 | |
| | 3 | .178 | .013 | .032 | |
| | 4 | .250 | .013 | .032 | |
| | 5 | .392 | .013 | .032 | |
| | 6 | .696 | .013 | .032 | |
| | 7 | 1.57 | .027 | .042 | |
| | 8 | 2.78 | .027 | .042 | |
| | 9 | 4.00 | .027 | .042 | |
| | 10 | Base | .027 | .042 | On Sting |

| PART NO. | NAME | NO. RQD. | MATERIAL DESC. | MATERIAL SPEC. | WEIGHT |
|---|---|---|---|---|---|
| | | | | | |

ALL DIMENSIONS IN INCHES
LIMIT ON DIMENSIONS — UNLESS OTHERWISE NOTED
ANGULAR ± ½°
FRACTIONAL ± 1/32
DECIMAL ± .010

NUMBERS ARE SURFACE ROUGHNESS IN MICROINCHES
R ROUGH MACHINE FINISH
16 FINISH GRIND
250 SMOOTH MACHINE FINISH
2 FINE GRIND, LAP
40 ROUGH GRIND
¼ POLISH

FINISH

HEAT TREAT

CALIFORNIA INSTITUTE OF TECHNOLOGY

FIG. 2 STATIC PRESSURE MODEL

DRAWN BY
TRACED BY
CHECKED BY
APPROVED BY
DATE
SCALE FULL
COURSE NO.
DWG. NO.
SECTION NO.

DIETERICH-POST CLEARPRINT 1000H

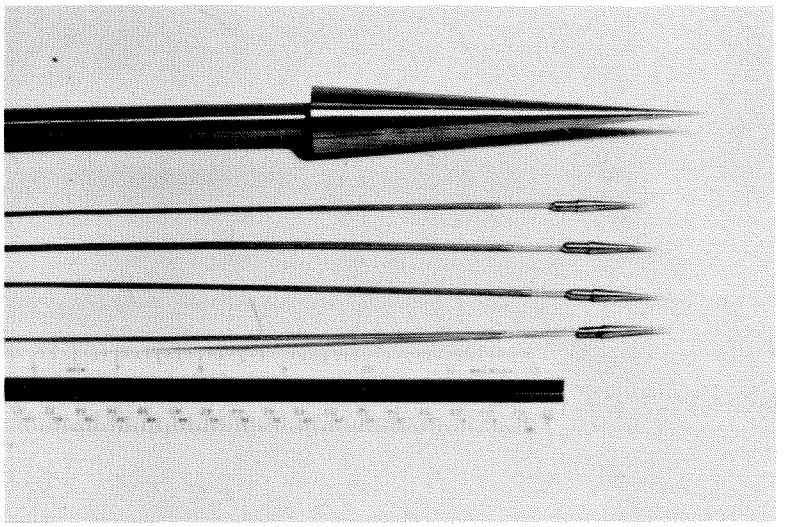

Fig. 3 STATIC PRESSURE MODEL

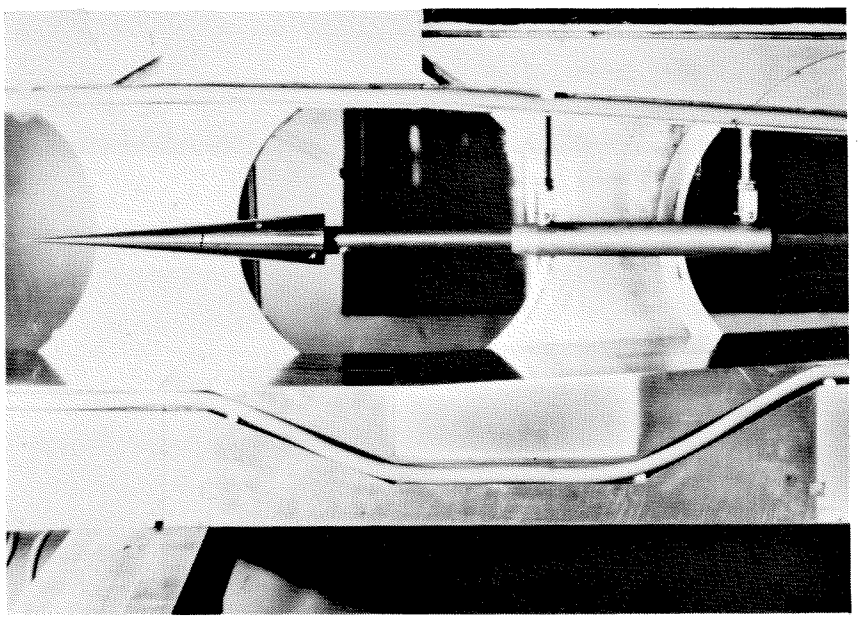

Fig. 4 STATIC PRESSURE MODEL IN HYPERSONIC TUNNEL

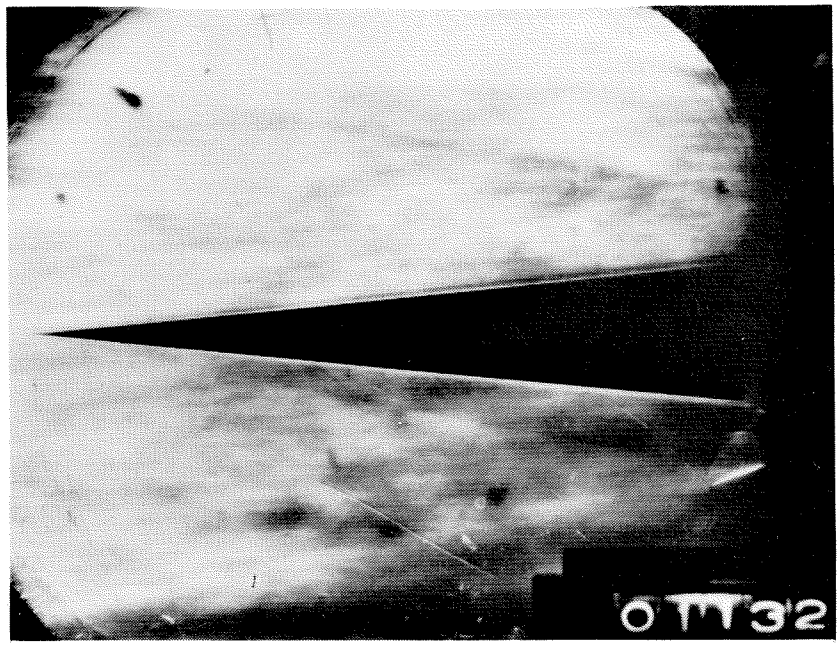

Fig. 5 SCHLIEREN PHOTOGRAPH OF CONE

Fig. 6(a)
Tip No. #1

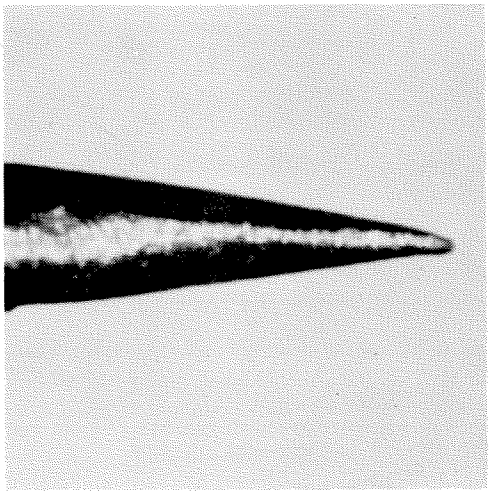

Fig. 6(b)
Tip No. #2

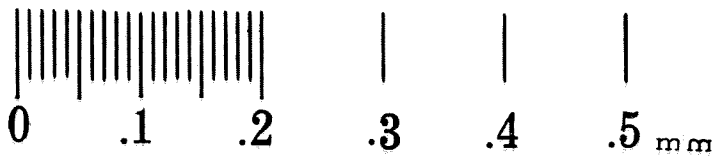


Magnification 160x

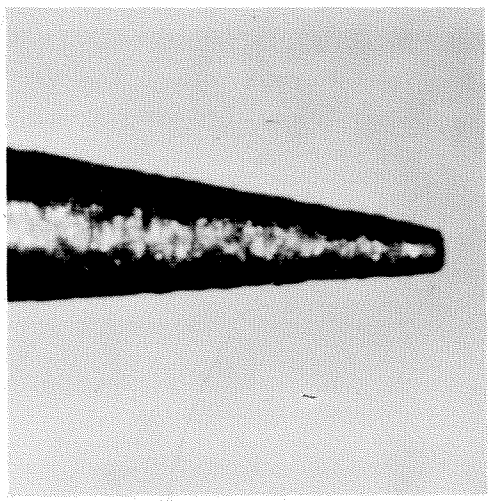

Fig. 6(b)
Tip No. #3

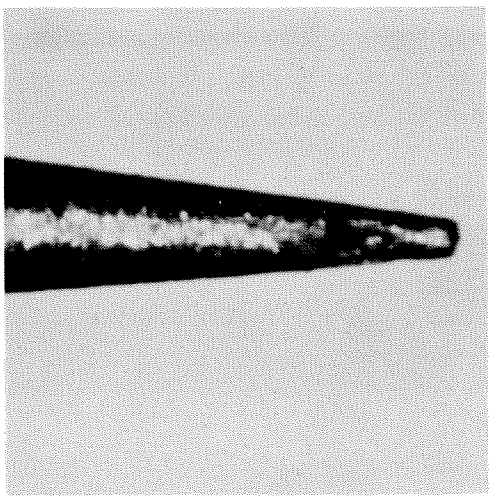

Fig. 6(d)
Tip No. #5

Fig. 6 MICROPHOTOGRAPHS OF CONE TIPS

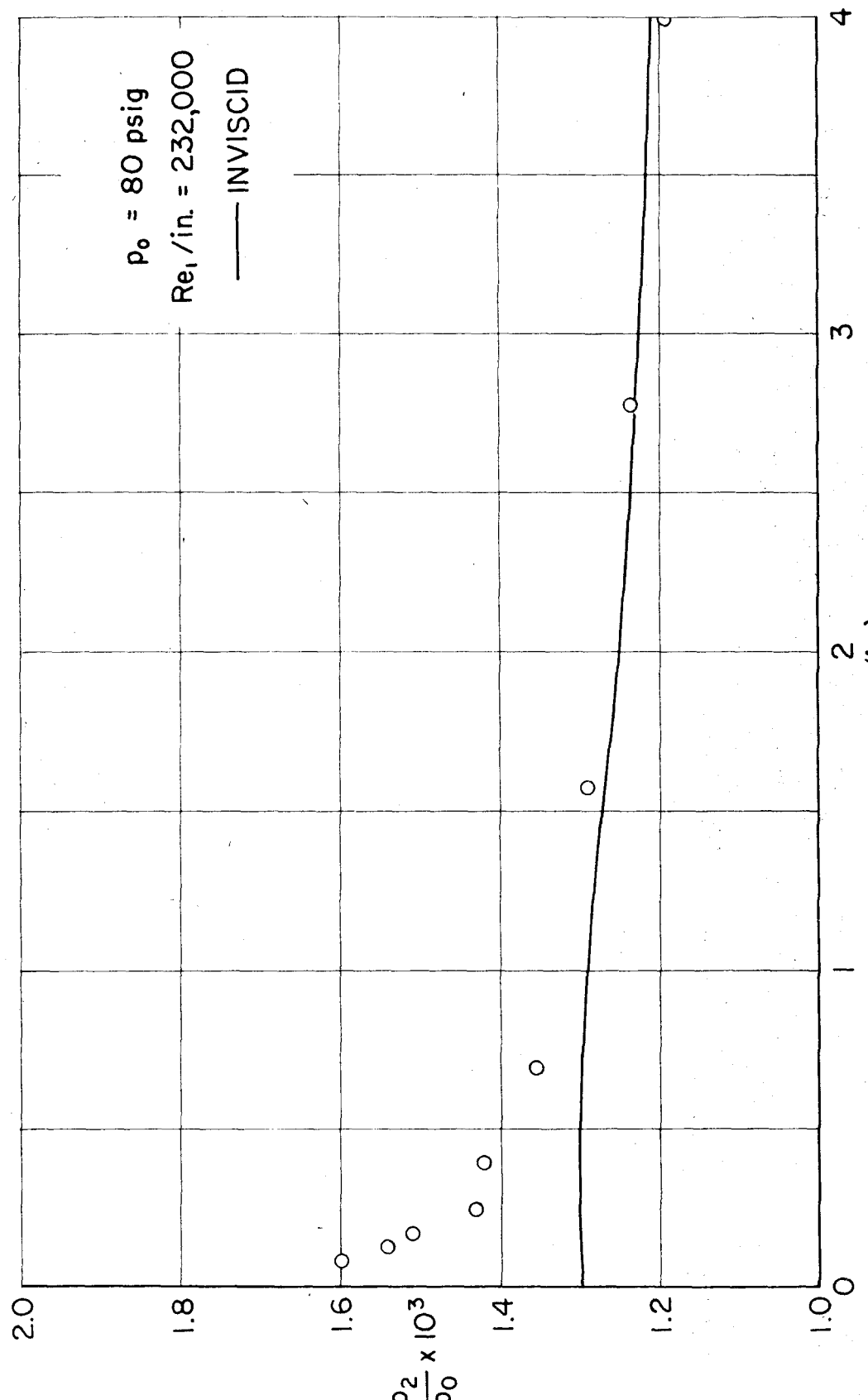


FIG. 7 STATIC PRESSURE RATIO VERSUS DISTANCE

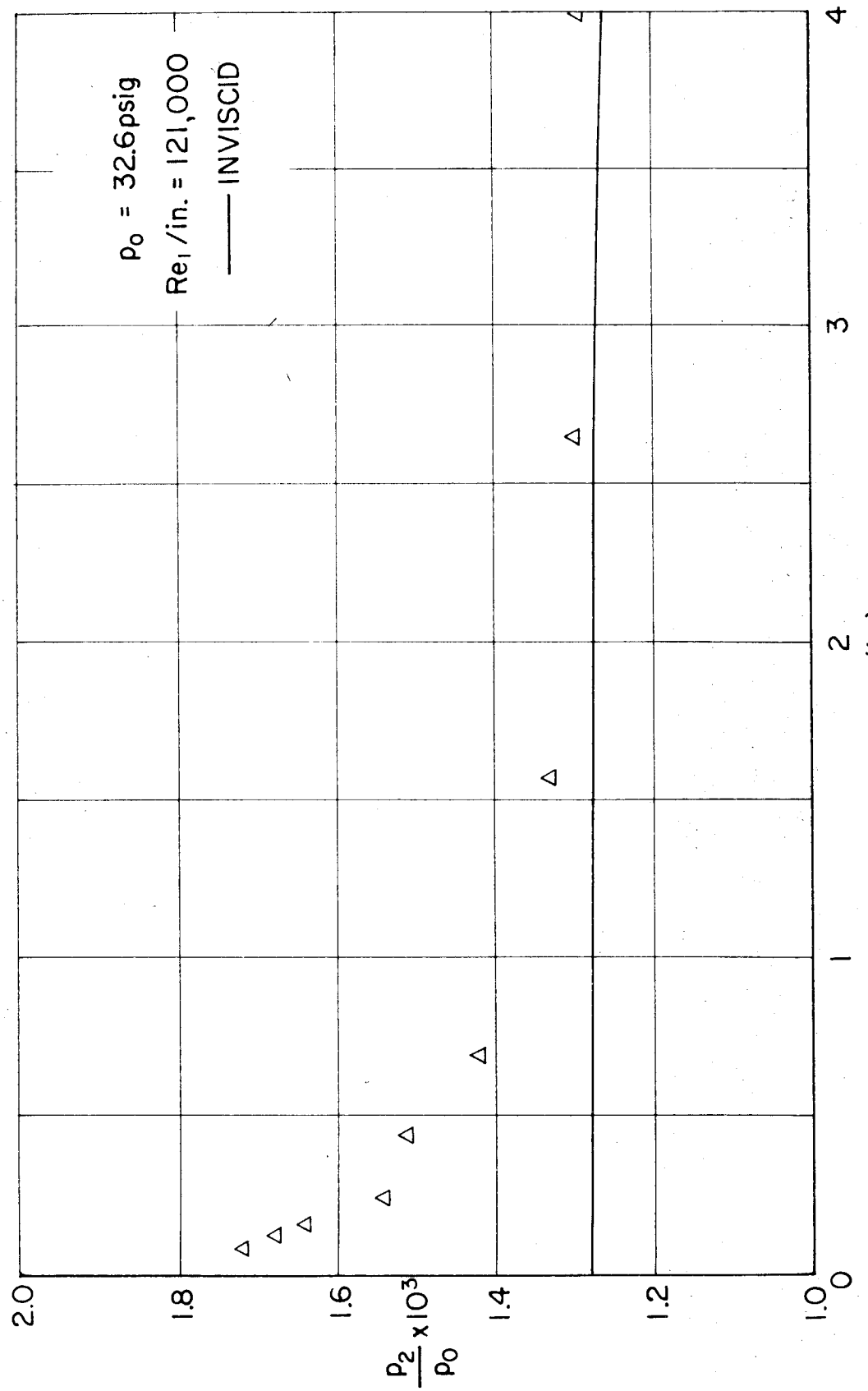


FIG. 8 STATIC PRESSURE RATIO VERSUS DISTANCE

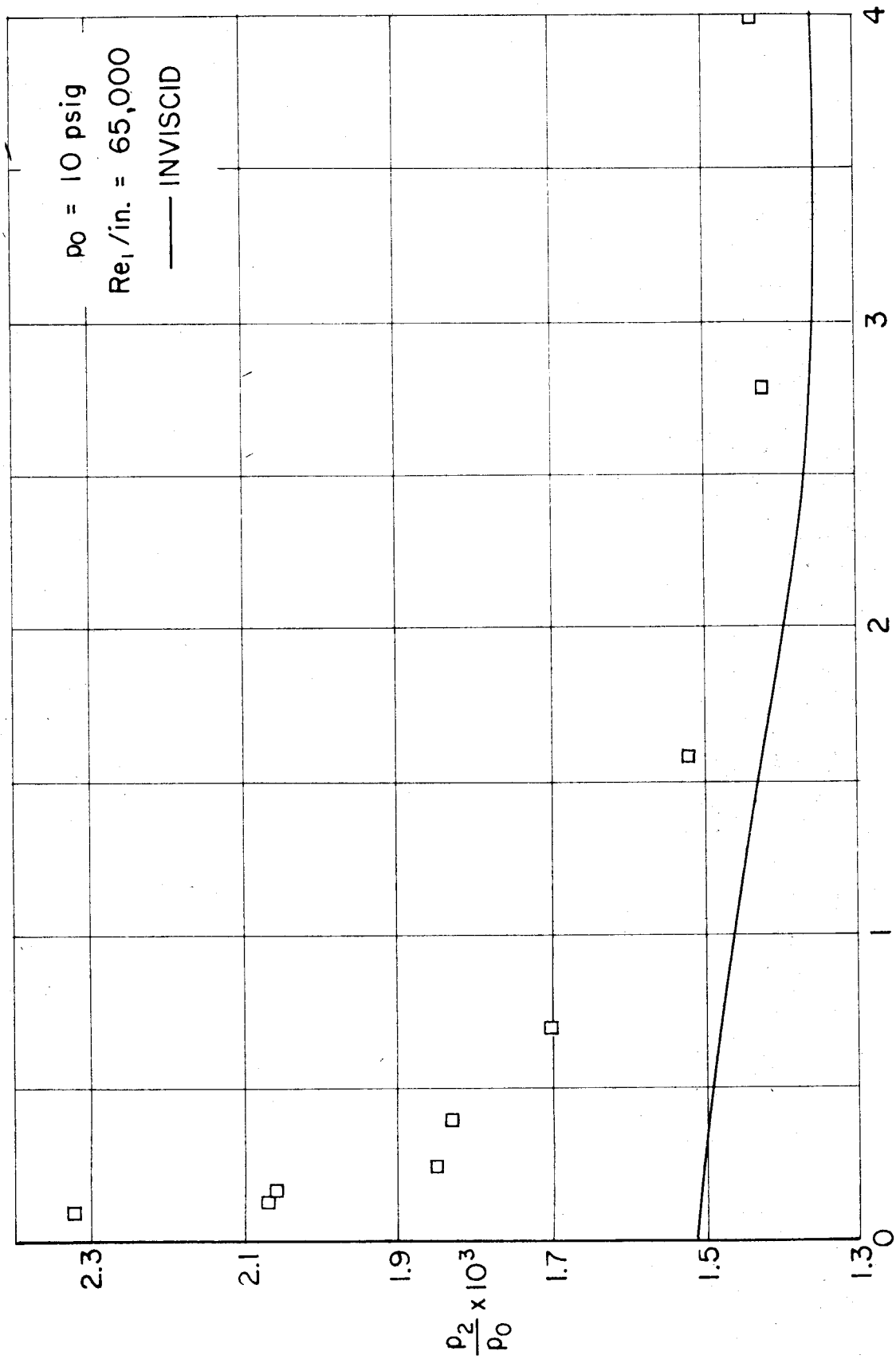


FIG. 9 STATIC PRESSURE RATIO VERSUS DISTANCE

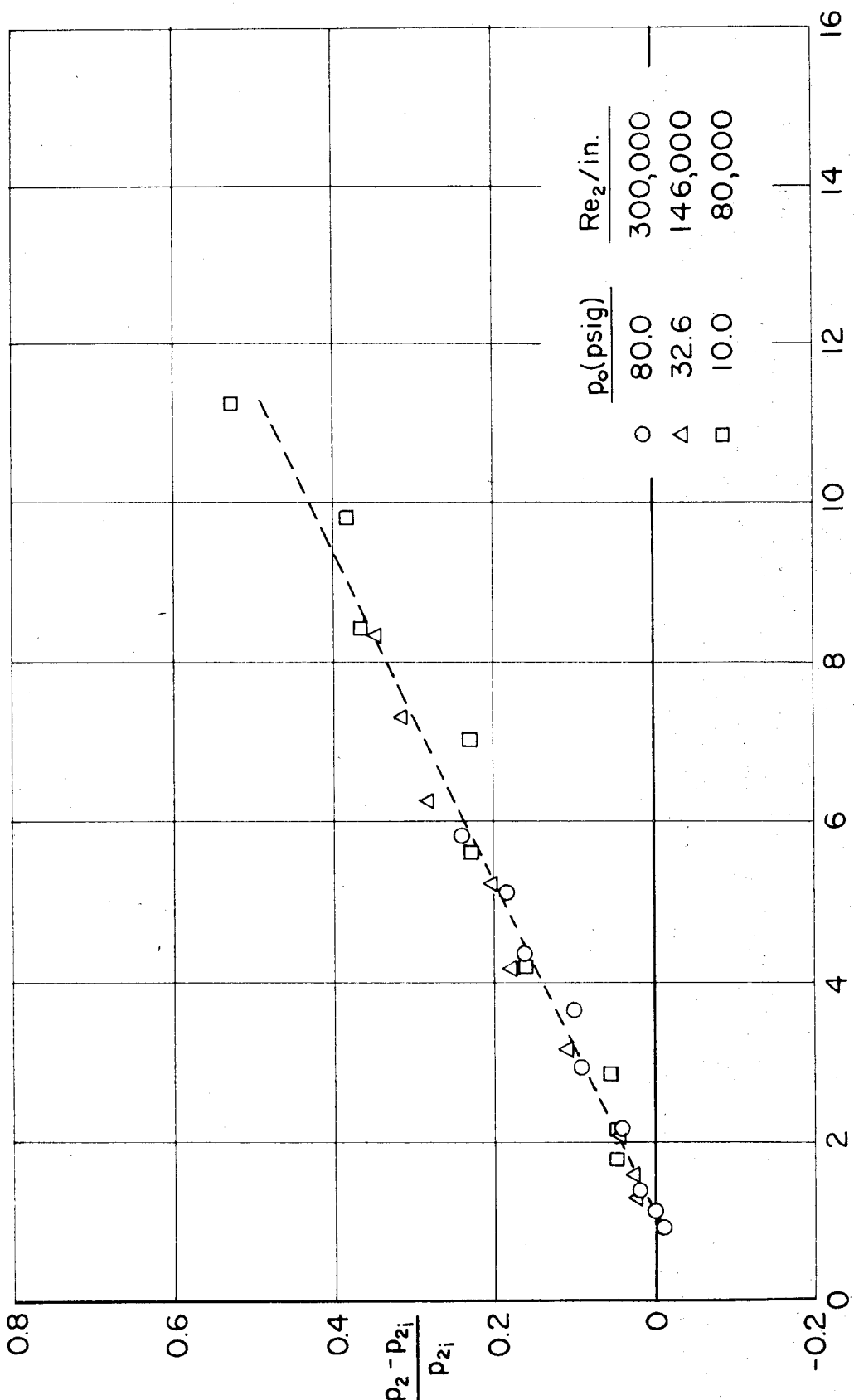


FIG. 10 INDUCED PRESSURE INCREMENT VERSUS $\frac{1}{\sqrt{Re_{x_2}}}$

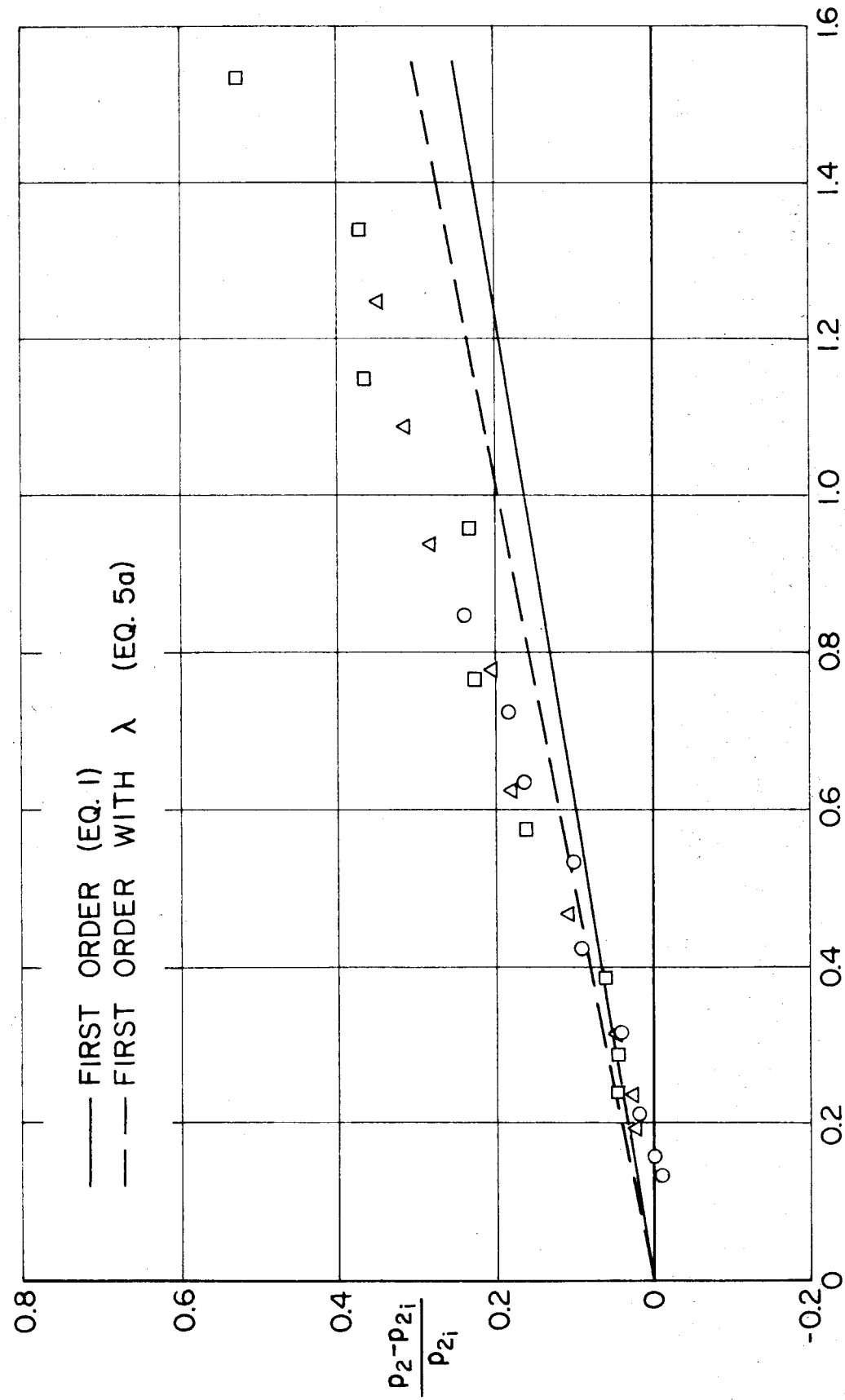


FIG. 11 COMPARISON OF INDUCED PRESSURE WITH THEORY

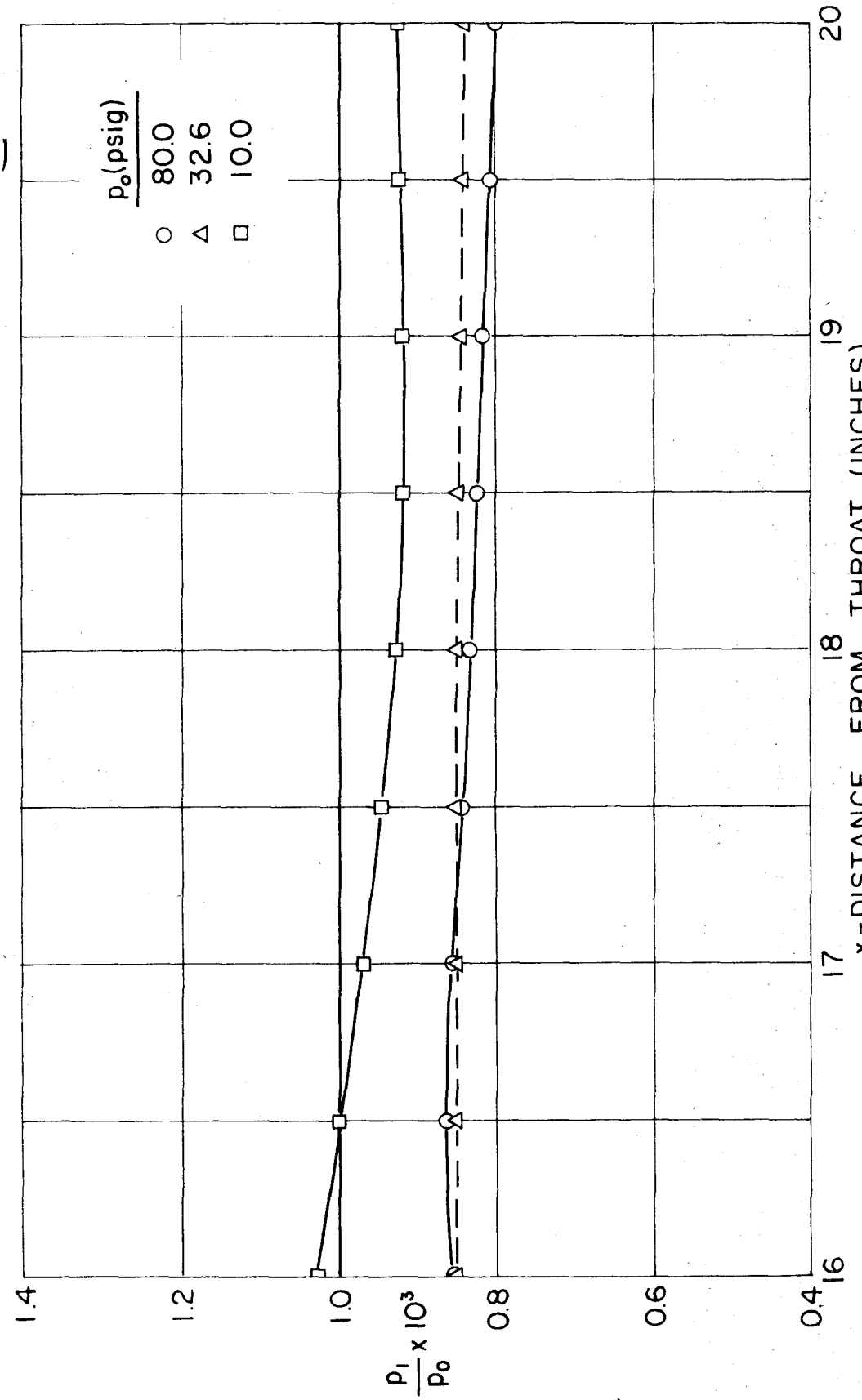


FIG. 12 STATIC PRESSURE RATIO ALONG TUNNEL CENTER LINE (TUNNEL EMPTY)